Oligomycin inhibits store-operated channels by a mechanism independent of its effects on mitochondrial ATP

Jwa Hwa CHO*, M. BALASUBRAMANYAM*, Galina CHERNAYA*, Jeffrey P. GARDNER*, Abraham AVIV*, John P. REEVES*, Pauline G. DARGIS† and Edward P. CHRISTIAN†‡

*Hypertension Research Program and Departments of Pediatrics and Physiology, University of Medicine and Dentistry–New Jersey Medical School, 185 South Orange Avenue, Newark, NJ 07103, U.S.A., and †Department of Pharmacology, Zeneca Pharmaceuticals, Wilmington, DE 19850-5437, U.S.A.

Inhibitors of mitochondrial oxidative metabolism have been proposed to interfere with Ca^{2+} influx mediated by store-operated channels (SOC), secondary to their effects on ATP production. We assessed SOC activity by $^{45}Ca^{2+}$ influx and fluorimetric measurements of free Ca^{2+} or Mn^{2+} quench in thapsigargin-treated Chinese hamster ovary cells and Jurkat T-cells, and additionally by electrophysiological measurements of the Ca^{2+}-release-activated Ca^{2+} current (I_{crac}) in Jurkat T-cells. Various mitochondrial antagonists were confirmed to inhibit SOC. However, the following evidence supported the proposal that oligomycin, in particular, exerts an inhibitory effect on SOC in addition to its known actions on mitochondria and Na^+-pump activity: (i) the concentrations of oligomycin required to inhibit SOC-mediated Ca^{2+} influx or I_{crac} (half-inhibitory concentration $\sim 2\ \mu M$) were nearly 50-fold higher than the concentrations that blocked mitochondrial ATP production; (ii) the rank order of potency of oligomycins A, B and C for decreasing SOC-mediated Ca^{2+} influx or I_{crac} differed from that known for inhibition of mitochondrial function; (iii) oligomycin blocked I_{crac} under voltage clamp and with intracellular Na^+ and K^+ concentrations fixed by dialysis from the patch pipette, arguing that the effect was not secondary to membrane polarization or pump activity; and (iv) fixing the cytosolic ATP concentration by dialysis from the patch pipette attenuated rotenone- but not oligomycin-mediated inhibition of I_{crac}. Oligomycin also blocked volume-activated Cl^- currents, a profile common to some other known blockers of SOC that are not known mitochondrial inhibitors. These findings raise the possibility that oligomycin interacts directly with SOC, and thus may extend the known pharmacological profile for this type of Ca^{2+}-influx pathway.

INTRODUCTION

A variety of hormonal agonists, growth factors and specific antigenic stimuli transduce their signals through the phosphoinositide cascade, leading to an elevation of cytosolic inositol 1,4,5-trisphosphate (IP_3). Consequent activation of an IP_3-receptor–channel complex in the endoplasmic reticulum membrane then releases Ca^{2+} from this store and produces a transient elevation of the intracellular free Ca^{2+} concentration ($[Ca^{2+}]_i$). In many cells, the release of Ca^{2+} from IP_3-sensitive stores subsequently leads to activation of a Ca^{2+}-influx pathway in the plasma membrane, producing a sustained elevation of $[Ca^{2+}]_i$ in response to the stimulus. This latter pathway was first denoted as capacitative Ca^{2+} entry [1], but in an effort to support standardization of terminology, it will be referred to here as Ca^{2+} influx mediated by store-operated channels (SOC). SOC-mediated Ca^{2+} influx can be elicited by treating cells with thapsigargin (Tg), a selective inhibitor of the sarco(endo)plasmic reticulum Ca^{2+}-ATPase [2]; Tg causes a gradual loss of Ca^{2+} from the IP_3-sensitive stores and consequently activates this Ca^{2+}-influx pathway [3]. Whole-cell patch-clamp studies have revealed Ca^{2+} currents mediated by SOC in some cell types. In particular, these small Ca^{2+} selective currents, which depend on depletion of IP_3-sensitive stores, have been characterized in mast cells [4] and in T-lymphocytes [5–8], where they have been designated as the Ca^{2+}-release-activated Ca^{2+} current (I_{crac}; [4,8]). I_{crac} is distinct from voltage-gated Ca^{2+} currents in excitable cell types. For instance, I_{crac} is voltage-independent, exhibits greater permeability to Ca^{2+} than to Ba^{2+}, and is not affected by the known organic pharmacological blockers of voltage-gated Ca^{2+} channels.

Convincing evidence is available that the sustained elevation of $[Ca^{2+}]_i$ mediated by SOC is a critical component of the physiological response to humoral signals, and is responsible for refilling of IP_3-sensitive stores with Ca^{2+} [1], for maintaining $[Ca^{2+}]_i$ oscillations [9] and for inducing Ca^{2+}-dependent gene expression [10]. These critical Ca^{2+}-influx pathways thus appear to be not only obligatorily linked to Ca^{2+} store depletion but also highly regulated by a variety of factors, although these mechanisms and their cellular heterogeneity remain poorly defined. Multiple hypotheses concerning the activation and modulation of SOC have been suggested, but no consensus has yet been reached [11–13].

One proposed regulator of SOC is the intracellular adenine or guanine nucleotide level, based on the observation that chemically diverse anti-mitochondrial agents, including oligomycin, inhibit SOC-mediated Ca^{2+} influx in Jurkat and other cell types [14–16]. In the present study we have examined the effects of oligomycin and other blockers of mitochondrial ATP production on SOC in Jurkat cells and Chinese hamster ovary (CHO) cells using a variety of techniques, including fluorimetric measurement of $[Ca^{2+}]_i$, $^{45}Ca^{2+}$ or Mn^{2+} uptake, and whole-cell patch-clamp electrophysiology. Some of our results support the notion that

Abbreviations used: $[Ca^{2+}]_i$, intracellular free Ca^{2+} concentration; CHO cells, Chinese hamster ovary cells; HBS, Hepes-buffered solution; $I_{Cl(Vol)}$, volume-activated chloride current; I_{crac}, Ca^{2+}-release-activated Ca^{2+} current; IP_3, inositol 1,4,5-trisphosphate; NPPB, 5-nitro-2-(3-phenylpropylamino)benzoic acid; PSS, physiological salts solution; SOC, store-operated channel(s); Tg, thapsigargin.

‡ To whom correspondence should be addressed.

the intracellular ATP level positively regulates SOC. However, these diverse experimental approaches also provide convergent evidence that oligomycin inhibits store-dependent Ca^{2+}-influx pathways with low-micromolar potency independent of its effects on ATP production.

Some of the data described here have previously been published in abstract form [17].

MATERIALS AND METHODS

Materials

Oligomycin was obtained from Sigma (St. Louis, MO, U.S.A.; cat. no. O4876) and was a mixture of oligomycins A, B and C (approx. 65 % oligomycin A); an average mass of 791 g/mol was assumed for computing concentrations. Oligomycins A, B and C (Sigma) were also used individually in certain experiments, where indicated. All other biochemicals were from Sigma. ATP levels were measured using a firefly-luciferase kit supplied by Calbiochem (San Diego, CA, U.S.A.).

Cells

CHO cells were obtained from the American Type Culture Collection (Rockville, MD, U.S.A.; no. CCL 61) and were transfected with the mammalian expression vector pcDNA3 (Invitrogen, San Diego, CA, U.S.A.) containing no insert; they are routinely used as control cells in one of our laboratories (J. P. R.) for studies of transfected CHO cells expressing the cardiac Na^+/Ca^{2+} exchanger. The cells were grown in Iscove's modified Dulbecco's medium containing 10 % (v/v) fetal calf serum and 500 mg/ml geneticin (G418), as described [18]. The human leukaemic T-cell line Jurkat (clone E6-1; no. TIB 152) was also obtained from the American Type Culture Collection. The cells were maintained in RPMI 1640 medium supplemented with 10 % (v/v) fetal calf serum. The Jurkat cells used in electrophysiological studies were maintained in exponential growth phase between 0.1×10^6 and 1.5×10^6 cells/ml.

Measurement of $[Ca^{2+}]_i$

CHO cells were grown to confluence in 75 cm^2 plastic culture flasks. The cell monolayer was washed three times with physiological salts solution (PSS) containing (in mM) 140 NaCl, 5 KCl, 1 $MgCl_2$, 10 glucose and 20 Mops, buffered to pH 7.4 (37 °C) with Tris. The cells were released from the flask by the addition of 5 mM EDTA to the PSS, centrifuged (700 ***g***; 1 min) and resuspended twice in PSS containing 1 mM $CaCl_2$. Aliquots of cells were loaded with 3 μM fura-2/AM for 30 min in PSS/1 mM $CaCl_2$; in some experiments, 5 μM fura-2/AM was used. Sulfinpyrazone (0.25 mM) was included to retard transport of fura-2 out of the cells. After loading, individual aliquots of cells were centrifuged, resuspended and incubated for 1 min in 100 μl of PSS containing 0.3 mM EGTA and 200 nM Tg. The cells were then centrifuged again and resuspended in PSS (pH 8.0), and placed in a fluorescence cuvette. $CaCl_2$ (1 mM) was added after 30 s and fluorescence was monitored at 505 nm emission with excitation at 340 nm and 380 nm in a FluoroMax spectrofluorimeter (SPEX Industries, Edison, NJ, U.S.A.). Experiments with the CHO cells were conducted at pH 8.0 to facilitate comparison with the $^{45}Ca^{2+}$ uptake assay (cf. below). Calibration of the 340/380 nm ratios was accomplished by adding 10 mM digitonin to the cuvettes in the presence of 1 mM $CaCl_2$ for determination of R_{max}, followed by addition of 3 mM EGTA for the determination of R_{min} according to the formula of Grynkiewicz et al. [19]. Autofluorescence, determined from the fluorescence of unloaded cells, was subtracted from all raw data prior to $[Ca^{2+}]_i$ calculations.

For fura-2 measurements with Jurkat cells, the cells were washed with Hepes-buffered solution (HBS) consisting of (in mM) 140 NaCl, 5 KCl, 1 $MgCl_2$, 10 glucose and 20 Hepes (pH 7.4). After centrifugation (200 ***g*** for 10 min), cells were resuspended in HBS containing 0.1 % fatty-acid-free BSA. Cells were incubated with 2 μM fura-2/AM and 0.25 mM sulfinpyrazone for 30 min at 37 °C. Treatment of Jurkat cells with Tg and subsequent monitoring of fluorescence was as described above for the CHO cells, except that 100 nM Tg was used, the preincubation time was 2 min and solutions were buffered with Hepes instead of Mops/Tris.

$^{45}Ca^{2+}$ uptake assay

Preliminary experiments with the CHO cells indicated that Tg stimulated $^{45}Ca^{2+}$ uptake only at pH values more alkaline than pH 7.4. All experiments with CHO cells were therefore conducted at pH 8.0. CHO cells were grown to confluence in 24-well plastic plates. Prior to the assay, the medium was replaced with PSS (pH 7.4), and the cells were incubated at 37 °C for 15 min. Tg (50 nM) was then added to the desired wells and the cells were incubated for an additional 15 min. To assay $^{45}Ca^{2+}$ uptake, the medium in each well was replaced with 200 μl of PSS (pH 8.0) containing 1 mM $^{45}CaCl_2$ (10 mCi/ml). After the desired interval, uptake was terminated by adding 1 ml/well of a solution composed of 100 mM $MgCl_2$, 10 mM $LaCl_3$ and 5 mM Mops (pH 7.4 with Tris). The termination medium was aspirated and the cells were washed two additional times by addition and aspiration of the termination medium. The cells were extracted with 1 ml of 0.4 M HNO_3, and the total radioactivity in the extract was measured.

Electrophysiological recordings

The standard whole-cell configuration of the patch-clamp technique was used for recordings [20]. Experiments were performed at room temperature (22–24 °C) in a static bath chamber mounted on the stage of a Nikon Diaphot inverted microscope. Pipettes were fabricated from thin-wall borosilicate glass (1.5 mm external diam., 1.12 mm internal diam.; World Precision Instruments, Sarasota, FL, U.S.A.) on a Flaming-Brown P-87 puller (Sutter Instruments, Novato, CA, U.S.A.) coated with Sylgard (Dow Corning, Midland, MI, U.S.A.) at the tip and polished to a DC resistance of 2–8 MΩ. The resistance of patch seals was > 10 GΩ. Following achievement of the whole-cell mode, uncompensated capacitive transients to a -1 mV step were analysed to determine cell capacitance and series resistance. Whole-cell capacitive transients were then nulled. Series resistance was usually less than 10 MΩ, and was not compensated for. Liquid junction potentials were also not corrected. Neither of these measurement errors were judged to affect the conclusions reached in this study. Membrane currents were amplified with either an Axopatch 1B or a 200A amplifier (Axon Instruments, Foster City, CA, U.S.A.). Voltage-clamp protocols were implemented and data acquisition performed with p-Clamp 6.0 software (Axon Instruments). Membrane currents were low-pass filtered at less than one-half the digitizing rate with an eight-pole Bessel filter (Frequency Devices, Haverhill, MA, U.S.A.) and digitized as computer files using p-Clamp software and a Digidata 1200 interface (Axon Instruments). An unfiltered record of currents was pulse-encoded to VCR tape for off-line analysis. p-Clamp software was used to measure current amplitudes, and Origin software (version 3.73; Microcal Inc., Northhampton,

MA, U.S.A.) was used to fit data to functions and to construct figures. Averaged data are expressed as means ± S.E.M. For statistical tests, $P < 0.05$ was taken to denote a significant effect.

Extracellular solutions were applied with a linear array of gravity-fed glass-lined tubes (100 μm internal diam.; Hewlett Packard Corp., Wilmington, DE, U.S.A.) controlled by a system of electronically switched solenoid valves (BME Systems, Baltimore, MD, U.S.A.). The tube containing the desired solution was placed less than one cell diameter from a cell prior to activating the solenoid. This system enabled re-equilibration of extracellular solutions in < 200 ms, based on the disappearance of I_{crac} upon switching to a Ca^{2+}-free external solution (see the Results section).

I_{crac} measurement

The compositions of solutions were as follows (in mM). Extracellular solution: 160 NaCl, 4.5 KCl, 2 $CaCl_2$, 1 $MgCl_2$, 5 D-glucose, 5 Hepes, pH adjusted to 7.4 with NaOH. Pipette solution: 140 caesium aspartate, 2 $MgCl_2$, 10 EGTA, 5 Hepes, pH adjusted to 7.2 with CsOH. The pipette solution was hypo-osmotic (~ 305 mOsm) relative to the extracellular solution (~ 320 mOsm). Equimolar Mg^{2+} was substituted for Ca^{2+} in 'Ca^{2+}-free' extracellular solution. When Mg_2ATP was added to the intracellular solution, the pH was re-adjusted to 7.2 with CsOH.

The voltage-clamp protocol to measure I_{crac} used a holding potential of 0 mV to minimize basal Ca^{2+} influx. Repetitive (0.5–1 Hz) 200 ms voltage steps to −100 mV, or 200 ms ramps between −100 and +20 or +40 mV, were delivered to monitor I_{crac}. Stable I_{crac} could generally be recorded for > 10 min using these protocols. Three to five current epochs were digitally averaged for all measurements. For voltage steps, current was measured 10–15 ms after step onset to remove any contribution of uncompensated capacitive transients. From this point, current was measured over a 2–3 ms digitally averaged interval. For voltage ramps, current was measured during a digitally averaged interval between −96 and −98 mV on the ramp. Leak current (i.e. residual current in Ca^{2+}-free solution) was always subtracted from total Ca^{2+} current recorded during steps or ramps to calculate the Ca^{2+}-selective I_{crac} amplitude. Data were rejected if the leak current varied by > 20 % during the experiment.

Measurement of volume-activated chloride current [$I_{Cl(Vol)}$]

The compositions of solutions were as follows (in mM). Extracellular solution: 160 NaCl, 4.5 KCl, 2 $CaCl_2$, 1 $MgCl_2$, 5 Hepes, pH adjusted to 7.4 with NaOH (~ 310 mOsm). Pipette solution: 160 NaCl, 2 $MgCl_2$, 0.1 $CaCl_2$, 1.1 EGTA, 4 Na_2ATP, 10 Hepes, pH adjusted to 7.2 with CsOH (~ 310 mOsm). To activate $I_{Cl(Vol)}$, the extracellular solution was made hypo-osmotic, relative to the intracellular solution, by diluting it by 20 % with distilled deionized water (resulting osmolality ~ 240 mOsm).

The voltage protocol used to monitor $I_{Cl(Vol)}$ delivered repetitive (0.5–1 Hz) 200 ms voltage ramps from −100 to +20 mV from a holding potential of −80 mV. Steady-state $I_{Cl(Vol)}$ could usually be recorded for > 10 min with this protocol. Current was measured and analysed in an analogous way to that described for I_{crac}, the main difference being that $I_{Cl(Vol)}$ was measured as a digital average between +17.8 and +19 mV on the ramp. Initial current measured by ramps before introducing the hypo-osmotic solution was taken as the leak current, and was subtracted from all measurements made in hypo-osmotic solutions in order to quantify the $I_{Cl(Vol)}$ amplitude.

RESULTS

Oligomycin inhibits SOC-mediated Ca^{2+} influx in CHO cells

Fura-2-loaded CHO cells were pretreated with 200 nM Tg as described in the Materials and methods section, and placed in a cuvette containing various concentrations of oligomycin. The $[Ca^{2+}]_i$ transient normally elicited by the P_{2U} purinergic agonist ATP [18] was completely abolished under these conditions, indicating that IP_3-sensitive stores had been depleted of Ca^{2+} by the Tg pretreatment (results not shown). As shown in Figure 1, the addition of 1 mM $CaCl_2$ produced a marked rise in $[Ca^{2+}]_i$, reflecting Ca^{2+} entry via SOC [compare with control trace (Ctr) in which Tg was omitted]. This rise in $[Ca^{2+}]_i$ was inhibited in a dose-dependent manner by oligomycin, with 50 % inhibition occurring between 1.5 and 3.0 μM.

As shown in Figure 2, Tg dramatically stimulated $^{45}Ca^{2+}$ uptake at alkaline pH, and this was inhibited by approx. 50 % by 3 μM oligomycin. These studies were conducted at pH 8.0 because we observed little, if any, effect of Tg on $^{45}Ca^{2+}$ uptake at pH 7.4. This finding was unexpected, since the effects of Tg on $[Ca^{2+}]_i$ and Mn^{2+} entry in fura-2-loaded CHO cells are nearly identical at pH 7.4 and alkaline pH. The reasons for this pH-dependence are not clear at present. To facilitate comparison of the fura-2 and $^{45}Ca^{2+}$-influx studies, all experiments with CHO cells described in the present paper were conducted at pH 8.0. It should be noted, however, that the inhibitory effects of oligomycin on SOC-mediated Ca^{2+} influx in fura-2-loaded CHO cells are essentially identical at pH 7.4 and 8.0.

The concentrations of oligomycin that blocked Ca^{2+} entry were much higher than those reported to inhibit mitochondrial ATP production in other cells (see, e.g., [21]). To examine this issue in CHO cells, we measured the effects of oligomycin on ATP levels in cells preincubated for 30 min in the absence of glucose; under these conditions, the cells are dependent on mitochondrial ATP synthesis for maintaining cellular ATP. Oligomycin concentrations as low as 0.04 μM decreased cellular ATP levels by 90 % within 10 min under these conditions (results not shown). Thus oligomycin inhibited mitochondrial ATP production in these cells at far lower concentrations than those necessary to decrease SOC-mediated Ca^{2+} entry. It is also

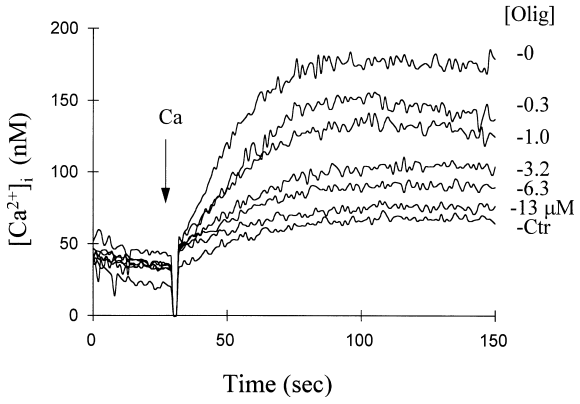

Figure 1 Inhibition of Tg-induced Ca^{2+} entry by oligomycin in CHO cells

Suspensions of CHO cells were loaded with fura-2, pretreated for 1 min with 200 nM Tg in PSS/0.3 mM EGTA, added to cuvettes containing PSS (0 time) and monitored for fura-2 fluorescence as described in the Materials and methods section. The cuvettes also contained the concentrations of oligomycin (Olig) indicated (μM). $CaCl_2$ (1 mM) was added at 30 s (arrow; Ca). For the control trace (Ctr), Tg was omitted during the 1 min preincubation and oligomycin was absent. Results of a representative experiment with a single batch of cells are shown.

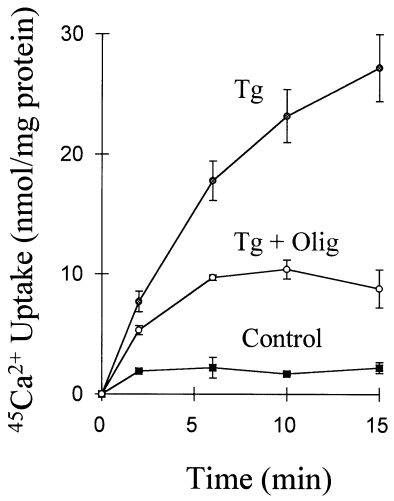

Figure 2 Effect of oligomycin on $^{45}Ca^{2+}$ uptake in Tg-treated CHO cells

Cells in 24-well plates were preincubated in PSS (pH 7.4) for 15 min with (○, ●) or without (■) 50 nM Tg. The PSS was then replaced (0 time) by PSS containing $^{45}Ca^{2+}$ (pH 8.0) and the cells were assayed for $^{45}Ca^{2+}$ uptake. Oligomycin (3.2 μM) was included for the final 10 min of preincubation and in the assay medium for the samples indicated by ○. Results are means ± S.E.M. of four experiments.

important to note that all the experiments reported here were carried out in the presence of 10 mM glucose; under these conditions, 3 μM oligomycin produces only a 30% decline in cellular ATP in CHO cells [22], the remainder presumably being supplied by glycolysis.

Oligomycin and SOC-mediated Ca^{2+} entry in Jurkat cells

Oligomycin also inhibited Tg-induced Ca^{2+} influx through SOC in Jurkat cells. As shown in Figure 3(a), the addition of Ca^{2+} to Tg-treated Jurkat cells resulted in a large transient rise in $[Ca^{2+}]_i$, followed by a stable plateau of elevated $[Ca^{2+}]_i$ at times > 90 s. Oligomycin decreased both the transient rise and the sustained $[Ca^{2+}]_i$ elevation in these cells, with a concentration-dependence similar to that seen in the CHO cells. All the results in Figure 3(a) were obtained with Tg-treated cells. As shown in Figure 3(b), when Tg was omitted during the preincubation in PSS/EGTA, a smaller $[Ca^{2+}]_i$ transient was observed than in the case of Tg-treated cells, and this transient was also inhibited by oligomycin (traces a and b in Figure 3b). However, when Jurkat cells were placed directly in the cuvette without the EGTA pretreatment, the rise in $[Ca^{2+}]_i$ upon the addition of extracellular Ca^{2+} was greatly decreased (trace c, Figure 3b) and was not inhibited by oligomycin; indeed, oligomycin slightly augmented the rise in $[Ca^{2+}]_i$ under these conditions (trace d, Figure 3b). Thus pretreatment with EGTA appears to activate Ca^{2+} entry in Jurkat cells even in the absence of Tg, presumably because the EGTA pretreatment partially depletes intracellular Ca^{2+} stores and leads to SOC activation. Consistent with this conclusion, Jurkat cells subjected to the EGTA pretreatment protocol (without Tg) showed a markedly decreased $[Ca^{2+}]_i$ transient upon discharge of intracellular Ca^{2+} stores by ionomycin compared with cells not exposed to EGTA (results not shown).

Oligomycin and Mn^{2+} entry through SOC

The rate of Mn^{2+} influx, as measured by the quenching of intracellular fura-2, is often used as an alternative measure of Ca^{2+}-channel activity in various cell types [23]. Mn^{2+} entry was accelerated in both CHO cells and Jurkat cells after treatment with Tg, and oligomycin antagonized this effect. The results for

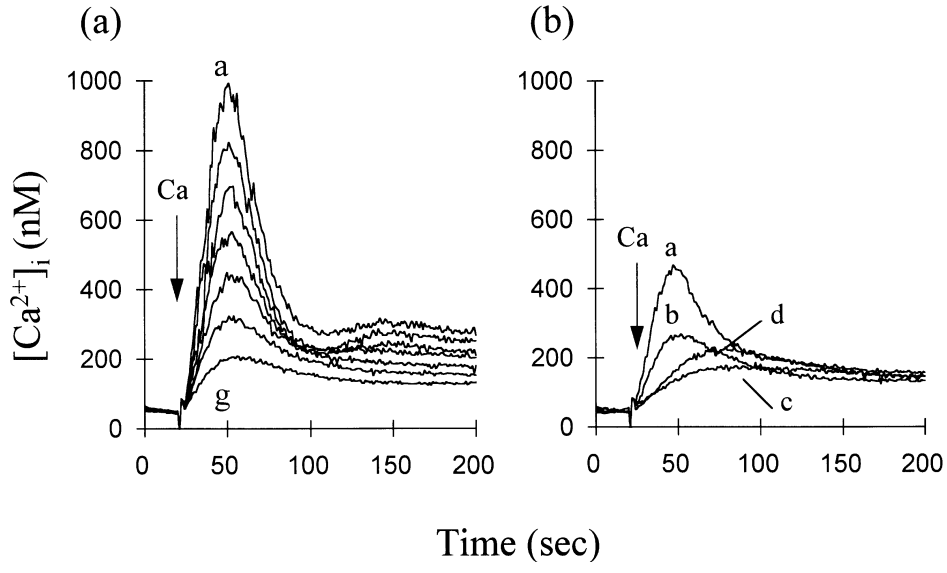

Figure 3 Inhibition of Tg-induced Ca^{2+} influx by oligomycin in Jurkat T-cells

(**a**) Fura-2-loaded Jurkat cells were pretreated for 2 min with 100 nM Tg in HBS/0.3 mM EGTA and then placed in cuvettes containing HBS and various concentrations of oligomycin (0 time). $CaCl_2$ (1 mM) was added as indicated by the arrow (Ca) and fura-2 fluorescence was monitored. Individual traces a–g (top to bottom) correspond to oligomycin concentrations of 0, 0.06, 0.25, 1.3, 3.2, 6.3 and 13 μM respectively. (**b**) Jurkat cells were preincubated for 2 min in HBS/0.3 mM EGTA in the absence of Tg and then added to cuvettes (0 time) with (trace b) or without (trace a) 13 μM oligomycin. For traces c and d, cells were centrifuged and resuspended directly in the cuvette medium (0 time) with (trace d) or without (trace c) 13 μM oligomycin (i.e. no EGTA or Tg pretreatment). For all traces, $CaCl_2$ (Ca; 1 mM) was added at the arrow.

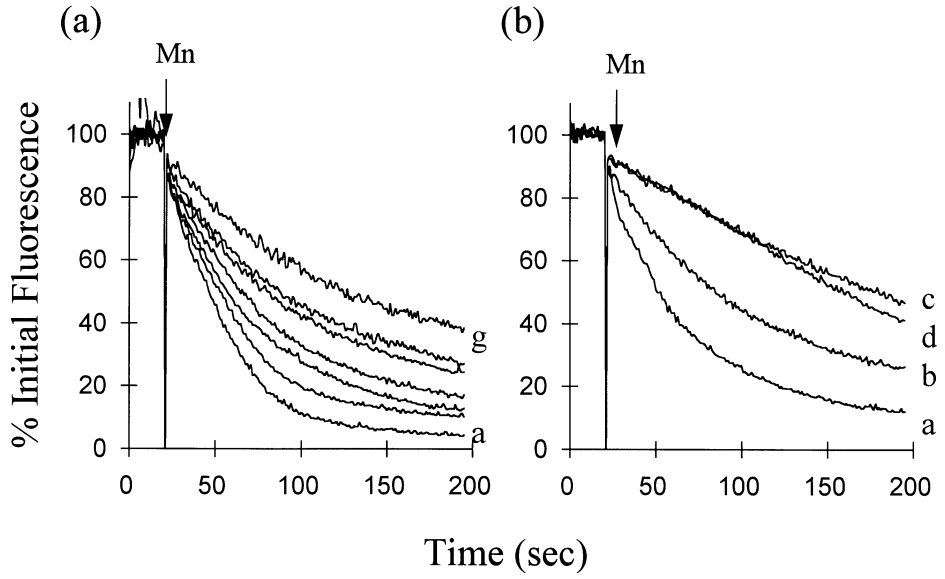

Figure 4 Effect of oligomycin on Tg-induced Mn^{2+} entry in Jurkat cells

The protocol and labelling of the traces are identical to those described for Figure 3, except that fura-2 fluorescence was monitored with excitation at 360 nM and Mn^{2+} (0.2 mM) was added where indicated. The rate of quenching of the fluorescence signal provides an index of the rate of Mn^{2+} entry.

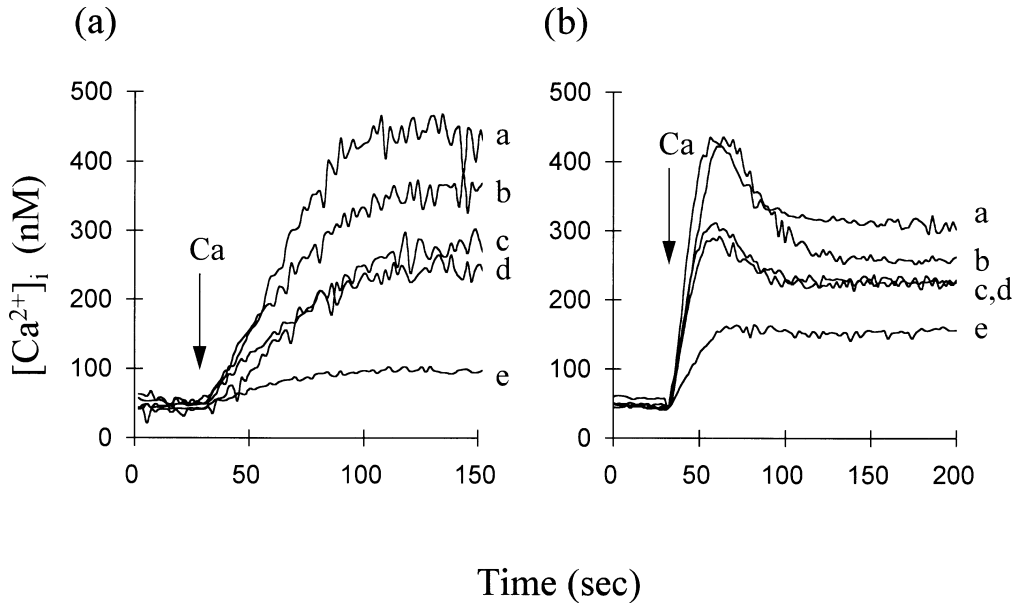

Figure 5 Inhibition of Tg-induced Ca^{2+} entry in CHO cells (a) and Jurkat T-cells (b) by rotenone, sodium azide, ouabain and oligomycin

(**a**) Fura-2-loaded CHO cells were pretreated for 1 min with 200 nM Tg in PSS/0.3 mM EGTA and then added to cuvettes (0 time) containing PSS and 3.2 μM oligomycin (trace e), 2 μM rotenone (trace d), 0.4 mM ouabain (trace c), 5 mM sodium azide (trace b) or no addition (trace a). $CaCl_2$ (Ca; 1 mM) was added at the arrow. (**b**) Jurkat T-cells were pretreated for 2 min with 100 nM Tg in HBS/0.3 mM EGTA and added to cuvettes (0 time) containing HBS and the same additions as shown in (**a**). Labelling of the traces and concentrations of agents are identical to those in (**a**), except that 10 mM sodium azide was used (trace b).

Jurkat cells are presented in Figure 4(a), where the rate of Mn^{2+} entry is indicated by the rate of decline in fura-2 fluorescence. As shown, oligomycin decreased the rate of Mn^{2+} entry with a concentration-dependence similar to that for its effects on the Tg-induced increase in $[Ca^{2+}]_i$ (the oligomycin concentrations for each trace are identical to those in Figure 3a). The data in Figure 4(b) are the counterpart to those in Figure 3(b). The results show that Mn^{2+} entry in Jurkat cells is partially accelerated by EGTA pretreatment alone (i.e. in the absence of Tg) and that this effect is antagonized by oligomycin (Figure 4b, traces a and b). As shown by traces c and d in Figure 4(b), oligomycin had no effect on Mn^{2+} entry in Jurkat cells not subjected to either EGTA or Tg pretreatment; the results are compatible with those presented in Figure 3(b).

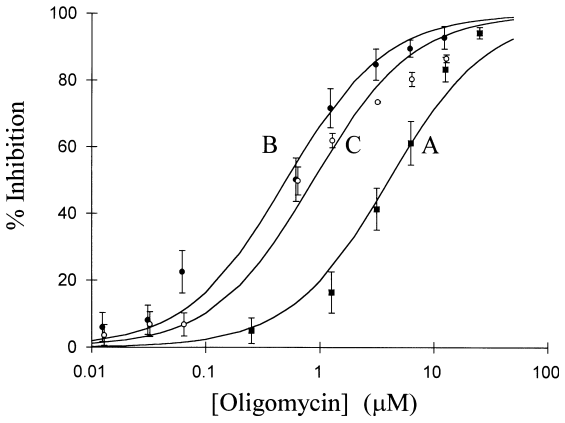

Figure 6 Effects of oligomycins A, B and C on Tg-induced Ca^{2+} influx in Jurkat T-cells

Jurkat cells were pretreated with 100 nM Tg in HBS containing 0.3 mM EGTA and added to cuvettes containing HBS and the indicated concentrations of oligomycin A, B or C. $CaCl_2$ (1 mM) was added and the peak increases in $[Ca^{2+}]_i$ were recorded for each oligomycin concentration and also for cells in the absence of oligomycin. The data presented are means $\pm$ S.E.M. ($n = 3$) for the percentage inhibition of the peak $[Ca^{2+}]_i$ values relative to the oligomycin-free controls. The solid curves were computed from the following equation: inhibition (%) $= 100 \times [Olig]/(K_{50} + [Olig])$, where [Olig] is the oligomycin concentration and K_{50} is the concentration giving 50% inhibition. K_{50} values obtained from the experimental values were 0.52 ± 0.08, 0.86 ± 0.13 and 4.0 ± 0.5 μM for oligomycins B, C and A respectively.

Comparison with other ATP inhibitors

Ca^{2+} entry through SOC is inhibited by a variety of mitochondrial inhibitors that appear to act by altering levels of cytosolic nucleotides [14–16]. We therefore compared the effects of oligomycin with those of other mitochondrial antagonists. The results for both CHO cells (Figure 5a) and Jurkat cells (Figure 5b) indicate that sodium azide (traces b) and rotenone (traces d) each partially inhibited the Tg-induced rise in $[Ca^{2+}]_i$, consistent with published results [14–16]. Neither agent was as effective as oligomycin in inhibiting Ca^{2+} entry (traces e), although all three agents blocked mitochondrial ATP production in CHO cells with equal effectiveness at the concentrations used, as assessed by measuring cellular ATP levels under glucose-free conditions (results not shown). Note that sodium azide has multiple known antagonistic effects on mitochondrial function: it acts as an uncoupler, it inhibits cytochrome oxidase and (like oligomycin) it inhibits the F_oF_1-ATPase [24]. Since oligomycin also inhibits the Na^+,K^+-ATPase [25], we compared its effects with those of ouabain. As shown in Figure 5 (traces c), ouabain partially inhibited the rise in $[Ca^{2+}]_i$ in both cell types, but again less effectively than oligomycin. These results suggest that oligomycin's inhibitory effects on the mitochondrial F_oF_1-ATPase and the Na^+,K^+-ATPase contribute to its inhibition of SOC-mediated Ca^{2+} entry. However, the experiments presented below argue that oligomycin exerts additional effects on SOC that are not related to inhibition of mitochondrial ATP production or Na^+ pump activity.

Oligomycin specificity

The oligomycin used in the above experiments was a mixture of oligomycins A, B and C (approx. 65% oligomycin A). We examined the effects of the individual oligomycins on the $[Ca^{2+}]_i$ response to Tg in Jurkat cells. As shown in Figure 6, the half-inhibitory concentrations for oligomycin B, C and A were 0.5, 0.9 and 4 μM respectively. A similar pattern was obtained for the CHO cells (results not shown). These results provide evidence that the effects of oligomycin on SOC were not exerted primarily through the mitochondrial F_oF_1-ATPase, since oligomycins A and B are equivalent in potency and oligomycin C is substantially less effective than either oligomycin A or B in inhibiting the F_oF_1-ATPase of rat liver mitochondria [26].

Effects of oligomycin on I_{crac}

Whole-cell patch-clamp studies were performed in Jurkat cells ($n = 63$) to characterize directly the effects of metabolic inhibitors on I_{crac}, which reflects the macroscopic current mediated by SOC [7] and is probably the exclusive pathway for store-dependent Ca^{2+} entry in these cells [6–8]. Following attainment of the whole-cell configuration with standard extracellular and pipette solutions, inward current measured during repeated (0.5 Hz) 200 ms steps to -100 mV from a 0 mV holding potential increased to an asymptotic level within 2–5 min (Figure 7a). This current was taken to be I_{crac}; the latency of its appearance presumably reflected both passive store depletion by the strongly Ca^{2+}-buffered (i.e. 10 mM EGTA, 0 mM Ca^{2+}) intracellularly dialysed solution, and signal transduction through an as yet undefined SOC activation pathway. Identity of the current as I_{crac} was based on an aggregate of hallmark properties corresponding to those previously documented for I_{crac} in Jurkat T-cells [5–8], and in close agreement with those that we have previously documented under conditions identical to those used here [27,28]. Briefly, these included low current density (1.31 ± 0.05 pA/pF at -100 mV; $n = 38$ cells recorded with control solutions), dependence on extracellular Ca^{2+} (Figures 7a and 7b), depolarized reversal potential (Figure 7b), inward rectification of the I–V relationship at hyperpolarized potentials (Figure 7b), apparent time- and voltage-independent activation, and rapid inactivation of current in the 100–200 ms time domain.

As shown in Figure 7, oligomycins A and B both blocked I_{crac} in Jurkat cells in a concentration-dependent manner. The extended recording in Figure 7(a) demonstrates the progressive block produced by increasing concentrations of oligomycin B ranging from 0.1 to 10 μM. Although blocking kinetics were not analysed systematically, this trace exemplifies the time course of the observed effects, which typically required from 20 s to 1 min to reach steady state over the concentration range tested. Figure 7(b) shows the effect of increasing oligomycin B concentrations on currents recorded during 200 ms voltage ramps between -100 and $+20$ mV in a different cell. These data indicate that oligomycin blocked a current with the signature Ca^{2+}-selectivity and depolarized reversal potential features of I_{crac} (see above).

Oligomycin A produced a concentration-dependent block of I_{crac} with similar characteristics, but with lower potency than oligomycin B (Figure 7c). Fits of averaged concentration–response data to a logistic function yielded IC_{50} values and slope factor coefficients (respectively) of 13.5 μM and 0.85 for oligomycin A, and 2.3 μM and 0.82 for oligomycin B. A two-way analysis of variance confirmed a significantly greater inhibition by oligomycin B over the concentration range tested ($P < 0.01$). These results were thus in close agreement with those obtained from the $[Ca^{2+}]_i$ measurements shown in Figure 6.

To address the question of whether oligomycin exerts an inhibitory effect on I_{crac} through a decrease in cellular ATP levels, its ability to block the current was examined in a series of experiments in which 2 mM Mg_2ATP was included in the pipette solution dialysing the cytosol (Figure 8). Although this exogenous source of ATP presumably maintained the cytosolic ATP at a fixed concentration, oligomycin B over the concentration range

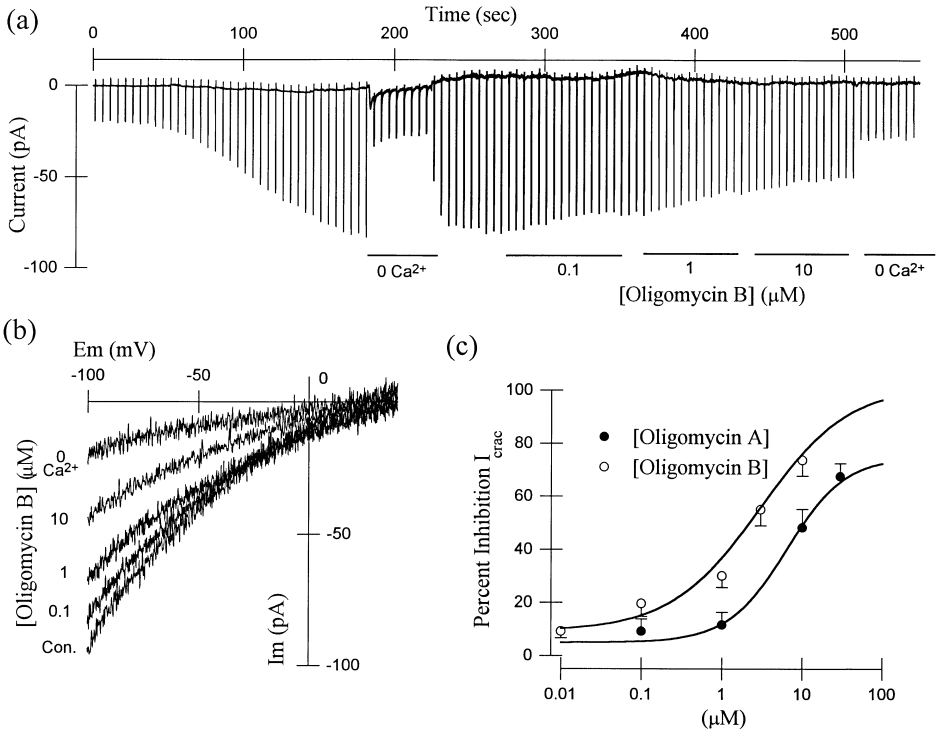

Figure 7 Effects of oligomycins A and B on I_{crac}

Whole-cell patch-clamp data were obtained from Jurkat cells using the solutions described for I_{crac} isolation in the Materials and methods section. (**a**) Continuous current record obtained from an experiment showing the concentration-dependent inhibitory effect of oligomycin B on I_{crac}. Negative deflections are responses to −100 mV, 200 ms steps (holding potential 0 mV) delivered at 0.2 Hz. The whole-cell configuration was achieved at '0 time'. Extracellular solutions containing 0 mM Ca^{2+} or oligomycin B concentrations were introduced as indicated by the bars. (**b**) Different experiment from that in (**a**) showing expanded superimposed current responses to 200 ms ramps from −100 to +40 mV (0 mV holding potential; traces not leak-subtracted) delivered at 0.2 Hz during superfusion with the indicated solutions; Im and Em are current and voltage respectively. Traces shown were obtained at steady state in each solution. (**c**) Averaged (means ± S.E.M.; n for data points ranges from 5 to 14) steady-state concentration–response data for the effects of oligomycins A and B on I_{crac} recorded using the protocol described in (**a**). Solid lines are fits of the data to the logistic function $-100/[1+(x/IC_{50})^h]+100$, where x is the oligomycin concentration, IC_{50} is the concentration producing a 50% I_{crac} block and h is the slope factor of the line. Parameters of fit were: oligomycin A, $IC_{50} = 13\ \mu M$, $h = 0.85$; oligomycin B, $IC_{50} = 2\ \mu M$, $h = 0.82$.

0.1–10 μM still blocked I_{crac} to an extent that did not differ significantly from that in experiments without ATP (Figure 8a; two-way ANOVA: $P = 0.094$).

In a separate set of experiments employing the same control conditions and protocols used for oligomycin in Figure 7, we found that the mitochondrial inhibitor rotenone also blocked I_{crac} in a concentration-dependent manner over the range 0.1–100 μM (one-half of current blocked at $\sim 47\ \mu$M; Figure 8b). However, in contrast with oligomycin B, inclusion of 2 mM ATP in the recording pipette decreased significantly the extent of inhibition of I_{crac} produced by rotenone over the 1–100 μM concentration range (Figure 8b; two-way ANOVA: $P < 0.01$). These data provided a positive control for the lack of effect of intracellular ATP addition on the oligomycin B-mediated inhibition of I_{crac} (Figure 8a), thereby further strengthening the conclusion that this inhibitory effect of oligomycin occurred independently of its known effects on mitochondrial ATP production.

One factor possibly complicating the ATP dialysis results with oligomycin and rotenone is a known inhibitory effect of protein kinase C activation on I_{crac} [29,30]. If the exogenously dialysed ATP served as a phosphate donor for protein kinase C, thereby inhibiting I_{crac}, as has been demonstrated previously in a rat basophilic leukaemia cell line (RBL-2H3) [29], this would have confounded the measurement of rotenone- or oligomycin-mediated inhibition under these conditions. Two separate parameters were thus measured to evaluate this potential complication. First, the mean peak I_{crac} density (prior to external drug application) in all cells dialysed with ATP was compared with the current density in cells recorded with control pipette solution. The peak I_{crac} density was 1.16 ± 0.10 pA/pF in ATP-dialysed cells ($n = 25$), and this did not differ significantly (unpaired t test; $P = 0.16$) from the peak current density of 1.31 ± 0.05 pA/pF in control cells ($n = 38$). Secondly, a separate set of control experiments was implemented to determine the extent to which the peak I_{crac} decayed after 5 min of recording (i.e. in the absence of any external drugs) in cells dialysed with control compared with ATP (2 mM)-containing pipette solution. The peak I_{crac} declined measurably under both conditions, but the percentage decline at 5 min after accessing the whole-cell recording mode did not differ significantly between the two groups (ATP-containing cells, $24 \pm 7\%$ decline, $n = 7$; control cells, $22 \pm 4\%$ decline, $n = 4$; unpaired t test: $P = 0.87$). Thus ATP dialysis itself affected neither the maximal current density that I_{crac} achieved nor the extent of slow decay of current in the time envelope encompassed by our pharmacological experiments.

Effects of oligomycin on $I_{Cl(Vol)}$

We evaluated the selectivity of oligomycin B for I_{crac} compared with $I_{Cl(Vol)}$ in Jurkat cells (Figure 9). In standard solutions for the isolation of $I_{Cl(Vol)}$ (described in the Materials and methods

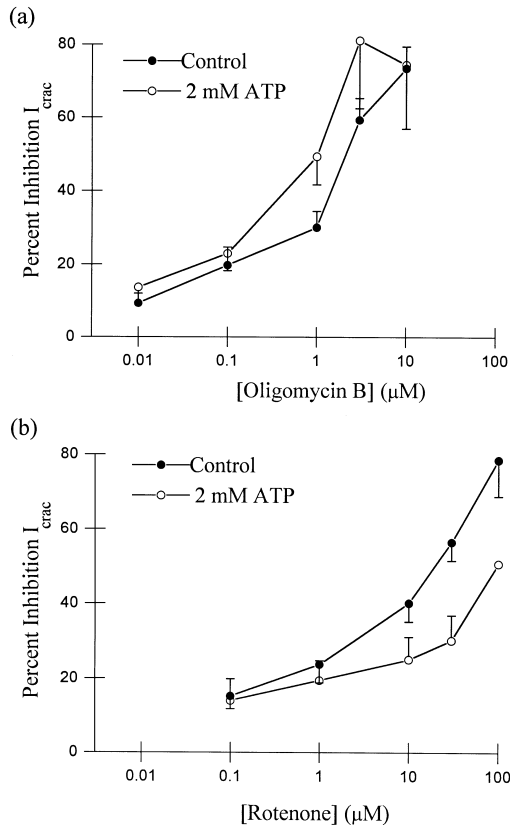

Figure 8 Effects of dialysed ATP on oligomycin-and rotenone-mediated I_{crac} inhibition

Mean ± S.E.M. steady-state concentration–response data are from whole-cell patch-clamp experiments in Jurkat cells using the solutions, voltage-clamp protocols and measurement procedures described for I_{crac} in the Materials and methods section. (**a**) Oligomycin B-mediated block of I_{crac} normalized as the percentage inhibition of total I_{crac} for experiments without (Control) and with 2 mM Mg_2ATP included in the pipette solution (*n* values for data points range from 4 to 14). (**b**) Rotenone-mediated concentration-dependent block of I_{crac} normalized as a percentage of control without and with 2 mM ATP in the pipette (*n* values for data points range from 3 to 10, except for a single point where the effect of 100 μM rotenone was measured with 2 mM ATP; $n = 1$).

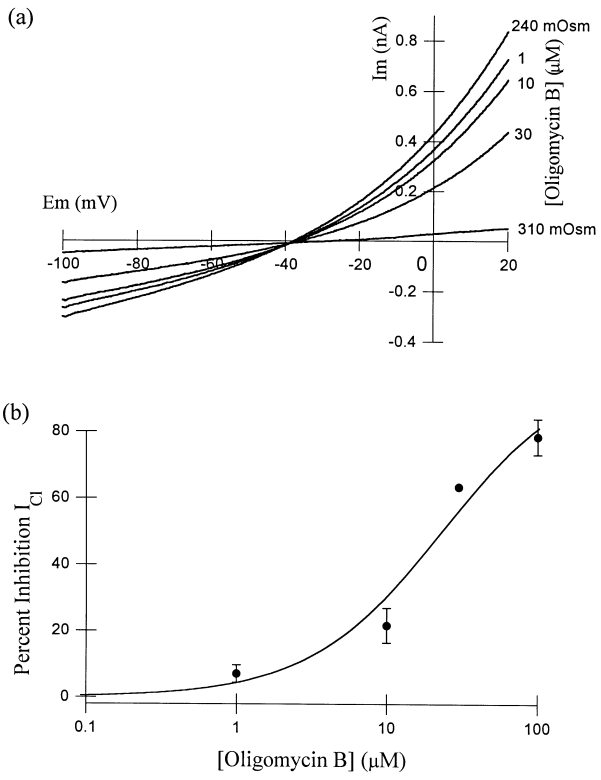

Figure 9 Effects of oligomycin B on $I_{Cl(Vol)}$

Whole-cell patch-clamp data were obtained from Jurkat cells using the solutions described for $I_{Cl(Vol)}$ isolation in the Materials and methods section. (**a**) Superimposed current responses to 200 ms ramps between −100 and +20 mV (holding potential −80 mV) delivered at 0.5 Hz during superfusion with the indicated solutions. The current was initially recorded prior to diluting the extracellular solution with deionized water (310 mOsm; leak current), after the current had reached steady state in dilute (240 mOsm) extracellular solution, and then after reaching steady state in each concentration of oligomycin B. Im and Em are current and voltage respectively. (**b**) Averaged (mean ± S.E.M.; *n* values for data points range from 2 to 5) steady-state concentration–response data for the effect of oligomycin B on $I_{Cl(Vol)}$ recorded using the protocol described for (**a**). $I_{Cl(Vol)}$ was measured as described in the Materials and methods section and normalized as the percentage inhibition of the maximum $I_{Cl(Vol)}$. The solid line is a fit of the data to the logistic function described in the legend to Figure 7. The parameters of fit were: $IC_{50} = 23$ μM; $h = 1.70$.

section), very little current was initially evident during 200 ms voltage ramps between −100 and +20 mV (Figure 9a; 310 mOsm). This was taken to be leak current and was subtracted from subsequent measurements. Dilution of the extracellular solution by 20 % with deionized water led to the development of an outwardly rectifying current that increased to an asymptotic amplitude over 1–2 min (Figure 9a; 240 mOsm). This current showed other features (reversal potential approx. −40 mV; dependence on extracellular chloride) in close agreement with the volume-activated chloride current previously characterized by Lewis et al. [31] under nearly identical recording conditions. $I_{Cl(Vol)}$ was blocked in a concentration-dependent manner by oligomycin B (1–100 μM), but with approximately an order of magnitude lower potency than I_{crac} (Figure 9a). The mean concentration–response data were well fitted by a logistic function, with an IC_{50} of 23 μM and a slope factor of 1.7 (Figure 9b). The oligomycin block of $I_{Cl(Vol)}$ occurred without a shift in the reversal potential (Figure 9a), arguing that the inhibition was specific for this current. Interestingly, in a separate set of experiments, rotenone was found to only slightly inhibit $I_{Cl(Vol)}$ at concentrations up to 100 μM (percentage block at 100 μM rotenone = 27 ± 4 %; $n = 4$; results not shown).

DISCUSSION

The results reported here show that oligomycin inhibits Tg-induced Ca^{2+} influx through SOC, as measured by $[Ca^{2+}]_i$ or $^{45}Ca^{2+}$ uptake, or Mn^{2+} quench of fluorescence, in both CHO and Jurkat cells (Figures 1–6). Moreover, patch-clamp studies likewise demonstrated that oligomycin blocks I_{crac} elicited by passive store depletion in Jurkat cells (Figures 7 and 8). Oligomycin is known to inhibit both the mitochondrial F_oF_1-ATPase and the Na^+,K^+-ATPase, and therefore could be inhibiting SOC secondary to effects such as ATP depletion or membrane depolarization. Indeed, evidence is available indicating that SOC-mediated Ca^{2+} influx is inhibited by either a decline in intracellular ATP [14,16] or a corresponding increase in ADP [15] brought about by a variety of diverse chemical agents that interfere with mitochondrial function.

Our results provide two lines of evidence consistent with the involvement of ATP or ATP/ADP ratios in regulating SOC.

First, we confirmed by both fluorimetric $[Ca^{2+}]_i$ measurement (Figure 5) and patch-clamp recording (Figure 8) that, in addition to oligomycin, other chemically diverse inhibitors of mitochondrial ATP production, such as rotenone and azide, inhibited SOC to varying degrees. Secondly, our patch-clamp studies revealed that the inhibitory effect of rotenone on I_{crac} was abrogated significantly by the inclusion of ATP in the recording pipette (Figure 8). Thus these findings confirm the conclusions of earlier work [14,16] by demonstrating directly with whole-cell recordings an ATP-dependent regulation of I_{crac}. However, our findings are difficult to reconcile with the recent patch-clamp results of Innocenti et al. [15]. Those investigators were only able to record inhibitory effects of metabolic drugs such as oligomycin and rotenone on I_{crac} under conditions where rat basophilic leukaemia cells were maintained at 37 °C and the pipette Ca^{2+}-buffering capacity was kept low. Such specific conditions were clearly not required in the present study to obtain I_{crac} inhibition in Jurkat T-cells with these same metabolic drugs in similar concentration ranges. Aside from the unlikely possibility that there is a fundamental difference in I_{crac} regulation by cell metabolism in these two cell types, we can offer no explanation for this apparent discrepancy at present.

The inhibitory effects of ouabain and mitochondrial antagonists on SOC-mediated Ca^{2+} influx (Figure 5) suggested that the inhibition of mitochondrial ATP production and Na^+,K^+-ATPase activity are likely to contribute to the oligomycin-mediated inhibition of SOC. However, our results also provided the following convergent observations arguing that additional mechanisms are involved: (i) the oligomycin concentrations required to inhibit Tg-induced Ca^{2+} entry and I_{crac} (0.5–10 μM; Figures 6 and 7) were 10–100-fold greater than those found to affect the F_oF_1-ATPase (< 0.04 μM), as assessed by the decrease in ATP in the absence of glucose; (ii) the rank order of potencies of the oligomycins for inhibiting SOC, as measured by both Tg-induced Ca^{2+} entry and I_{crac} (oligomycin B > C > A; Figures 6 and 7) differed from that previously established for inhibition of the F_oF_1-ATPase [26]; (iii) oligomycin blocked I_{crac} in Jurkat cells under conditions where the membrane potential was controlled by voltage clamp and the cell was dialysed with solutions of a defined ionic composition (Figure 7), arguing that neither membrane depolarization nor changes in cytosolic $[Na^+]$ or $[K^+]$ could account for the inhibitory effects; and (iv) the inhibition of I_{crac} by oligomycin was not reversed by the inclusion of 2 mM ATP in the patch pipette solution, but this manipulation significantly attenuated the inhibition of I_{crac} caused by rotenone (Figure 8). Taken together, these observations suggested that oligomycin inhibits SOC by mechanisms separate from or in addition to its known effects on the F_oF_1-ATPase or Na^+,K^+-ATPase.

The pharmacology of SOC pathways is not well developed at present. Known inhibitors of SOC-mediated Ca^{2+} influx or I_{crac} include inorganic ions such as La^{3+} and Cd^{2+} [4], and several relatively weak organic blockers such as SK&F 96365 [32,33], imidazole antimycotics such as econazole and miconazole [28,32,34,35], piperazine derivatives such as LU52396 [36], and diarylamine carboxylates such as 5-nitro-2-(3-phenylpropylamino)benzoic acid (NPPB) [37,38]. Our evidence for an inhibition of SOC by oligomycins at low-micromolar potency, independent of their mitochondrial effects, may therefore extend the pharmacological profile of these Ca^{2+}-influx pathways. Particularly notable in this regard was the difference between oligomycins B and A, where the sole structural difference of a carbonyl oxygen (oligomycin B) in place of two hydrogens (oligomycin A) produced an 8–9-fold increase in potency, as confirmed by both fura-2 measurements (Figure 6) and patch-clamp electrophysiology (Figure 7c). This result implies a considerable degree of structural specificity for the inhibitory effect on SOC. Further consideration of the structure–activity relationship of oligomycin analogues for SOC inhibition may extend our understanding of chemical features of a pharmacophore at which these compounds act.

Our finding that oligomycin B inhibited volume-regulated Cl^- currents in addition to SOC in Jurkat cells (Figure 9) is reminiscent of a similar pharmacological profile that has recently been established for NPPB [37,38]. Our own observations (J. P. Reeves, unpublished work) also indicate that NPPB and niflumic acid block SOC-mediated Ca^{2+} influx in CHO cells. The fact that oligomycin shares this pharmacological profile with these other agents that are not known mitochondrial inhibitors provides additional suggestive evidence that oligomycin has activity at these channels independent of its actions at mitochondria.

The growing number of agents that have been shown to inhibit both Cl^- channels and SOC raises the possibility that the two may share structural homology or common regulatory pathways as a basis for the pharmacological overlap. This is difficult to address at present, since no definitive molecular information is available on SOC, and their regulation is controversial. Alternatively, Cl^--channel activity may be directly involved in the modulation of SOC, although the mechanism of this involvement is unclear. The fact that NPPB and oligomycin block I_{crac} in voltage-clamp experiments argues against a critical role for Cl^- channels in supporting SOC-mediated Ca^{2+} influx by providing charge compensation for Ca^{2+} movements or maintaining membrane polarization [39].

In summary, oligomycin inhibited SOC-mediated Ca^{2+} influx in CHO and Jurkat cells, and blocked I_{crac} in Jurkat cells. Although the antagonistic effects of oligomycin on mitochondria and Na^+-pump activity may have contributed to the observed inhibition of SOC, a more direct interaction with these channels may also be involved.

This work was supported in part by N.I.H. Grant HL49932 to J.P.R. We thank Ms. K.T. Spence for critical comments on an earlier draft of this paper.

REFERENCES

1 Putney, J. W. (1990) Cell Calcium **11**, 611–624
2 Lytton, J., Westlin, M. and Hanley, M. R. (1991) J. Biol. Chem. **266**, 17067–17071
3 Jackson, T. R., Patterson, S. E., Thastrup, O. and Hanley, M. R. (1988) Biochem. J. **253**, 81–86
4 Hoth, M. and Penner, R. (1993) J. Physiol. (London) **465**, 359–386
5 McDonald, T. V., Premack, B. A. and Gardner, P. (1993) J. Biol. Chem. **268**, 3889–3896
6 Premack, B. A., McDonald, T. V. and Gardner, P. (1994) J. Immunol. **152**, 5226–5240
7 Zweifach, A. and Lewis, R. S. (1993) Proc. Natl. Acad. Sci. U.S.A. **90**, 6295–6299
8 Zweifach, A. and Lewis, R. S. (1995) J. Gen. Physiol. **105**, 209–226
9 Dolmetsch, R. E. and Lewis, R. S. (1994) J. Gen. Physiol. **103**, 365–388
10 Negulescu, P. A., Shastri, N. and Cahalan, M. D. (1994) Proc. Natl. Acad. Sci. U.S.A. **91**, 2873–2877
11 Berridge, M. J. (1995) Biochem. J. **312**, 1–11
12 Bode, H. P. and Netter, K. J. (1996) Biochem. Pharmacol. **51**, 993–1001
13 Lewis, R. S. and Cahalan, M. D. (1995) Annu. Rev. Immunol. **13**, 623–653
14 Gamberucci, A., Innocenti, B., Fulceri, R., Banhegyi, G., Giunti, R., Pozzan, T. and Benedetti, A. (1994) J. Biol. Chem. **269**, 23597–23602
15 Innocenti, B., Pozzan, T. and Fasolato, C. (1996) J. Biol. Chem. **271**, 8582–8587
16 Marriott, I. and Mason, M. J. (1995) Am. J. Physiol. **269**, C766–C774
17 Cho, J. W., Balasubramanyam, M., Aviv, A., Gardner, J. P. and Reeves, J. P. (1995) Biophys. J. **68**, A54
18 Pijuan, V., Zhuang, Y., Smith, L., Kroupis, C., Condrescu, M., Aceto, J. F., Reeves, J. P. and Smith, J. B. (1993) Am. J. Physiol. **264**, C1066–C1074
19 Grynkiewicz, G., Peonie, M. and Tsien, R. Y. (1985) J. Biol. Chem. **260**, 3440–3450

20 Hamill, O. P., Marty, A., Neher, E., Sakmann, B. and Sigworth, F. J. (1981) J. Biol. Chem. **391**, 85–100
21 Nieminen, A.-L., Saylor, A. K., Herman, B. and Lemasters, J. L. (1994) Am. J. Physiol. **267**, C67–C74
22 Condrescu, M., Gardner, J. P., Chernaya, G., Aceto, J. F., Kroupis, C. and Reeves, J. P. (1995) J. Biol. Chem. **270**, 9137–9146
23 Sage, S. O., Merritt, J. P., Hallam, T. J. and Rink, T. J. (1989) Biochem. J. **258**, 923–926
24 Vigers, G. A. and Ziegler, F. D. (1968) Biochem. Biophys. Res. Commun. **30**, 83–88
25 Fahn, S., Koval, G. J. and Albers, R. W. (1966) J. Biol. Chem. **241**, 1882–1889
26 Lardy, H. A., Witonsky, P. and Johnson, D. (1965) Biochemistry **4**, 552–554
27 Christian, E. P., Spence, K. T., Togo, J. A., Dargis, P. G. and Patel, J. (1996) J. Membr. Biol. **150**, 63–71
28 Christian, E. P., Spence, K. T., Togo, J. A., Dargis, P. G. and Warawa, E. (1996) Br. J. Pharmacol. **119**, 647–654
29 Parekh, A. B. and Penner, R. (1995) Proc. Natl. Acad. Sci. U.S.A. **92**, 7907–7911
30 Petersen, C. C. H. and Berridge, M. J. (1995) Biochem. J. **307**, 663–668
31 Lewis, R. S., Ross, P. E. and Cahalan, M. D. (1993) J. Gen. Physiol. **101**, 801–826
32 Mason, M. J., Mayer, B. and Hymel, L. J. (1993) Am. J. Physiol. **264**, C654–C662
33 Merritt, J. E., Armstrong, W. P., Benham, C. D., Hallam, T. J., Jacob, R., Jaxa-Chamiec, A., Leigh, B. K., McCarthy, S. A., Moores, K. E. and Rink, T. J. (1990) Biochem. J. **271**, 515–522
34 Alvarez, J., Montero, M. and Garcia-Sancho, J. (1992) FASEB J. **6**, 786–792
35 Alvarez, J., Montero, M. and Garcia-Sancho, J. (1991) Biochem. J. **274**, 193–197
36 Clementi, E., Martini, A., Stefani, G., Meldolesi, J. and Volpe, P. (1995) Eur. J. Pharmacol. **289**, 23–31
37 Gericke, M., Oike, M., Droogmans, G. and Nilius, B. (1994) Mol. Pharmacol. **269**, 381–384
38 Reinsprecht, M., Rohn, M. H., Spadinger, R. J., Pecht, I., Schindler, H. and Romanin, C. (1995) Mol. Pharmacol. **47**, 1014–1020
39 Kremer, S. G., Zeng, W., Hurst, R., Ning, T., Whiteside, C. and Skoreckik, K. L. (1995) J. Cell. Physiol. **162**, 15–25

Received 1 November 1996/7 February 1997; accepted 24 February 1997